ELSEVIER

Journal of Molecular Structure: THEOCHEM 850 (2008) 72–78

THEO CHEM

www.elsevier.com/locate/theochem

Addition reactions of nitrones on the reconstructed C(100)-2 × 1 surfaces

Zhiguo Wang [a,b], Honglun Wang [b], Yongjun Liu [a,b,*], Yourui Suo [b]

[a] School of Chemistry and Chemical Engineering, Shandong University, Jinan, Shandong 250100, China
[b] Northwest Institute of Plateau Biology, Chinese Academy of Sciences, Xining, Qinghai 810001, China

Received 23 March 2007; received in revised form 9 August 2007; accepted 17 October 2007
Available online 25 October 2007

Abstract

In this paper, the reactions of nitrone, *N*-methyl nitrone, *N*-phenyl nitrone and their hydroxylamine tautomers (vinyl-hydroxylamine, *N*-methyl-vinyl-hydroxylamine and *N*-phenyl-vinyl-hydroxylamine) on the reconstructed C(100)-2 × 1 surface have been investigated using hybrid density functional theory (B3LYP), Møller–Plesset second-order perturbation (MP2) and multi-configuration complete-active-space self-consistent-field (CASSCF) methods. The calculations showed that all the nitrones can react with the surface "dimer" via facile 1,3-dipolar cycloaddition with small activation barriers (less than 12.0 kJ/mol at B3LYP/6-31g(d) level). The [2+2] cycloaddition of hydroxylamine tautomers on the C(100) surface follows a diradical mechanism. Hydroxylamine tautomers first form diradical intermediates with the reconstructed C(100)-2 × 1 surface by overcoming a large activation barrier of 50–60 kJ/mol (B3LYP), then generate [2+2] cycloaddition products via diradical transition states with negligible activation barriers. The surface reactions result in hydroxyl or amino-terminated diamond surfaces, which offers new opportunity for further modifications.
© 2007 Elsevier B.V. All rights reserved.

Keywords: Nitrone; Carbon; Surface chemical reaction; Density functional calculations; Ab initio quantum chemical method and calculations

1. Introduction

Diamond has recently attracted much attention as a candidate material for the fabrication of electronic devices due to its unique properties such as high thermal conductivity, chemical inertness, high carrier mobility, wide band gap and multi-spectral optical transparency [1,2]. Similar to the surfaces of Si(100) and Ge(100), the bare diamond (100) undergoes a 2 × 1 reconstruction for which pairs of carbon atoms bind to each other via a strong σ bond and a weaker π bond, forming "dimers" [3–6]. Because of the nonplanar geometry of the surface dimers, the π-bond strength of the dimers is much weaker than their molecular analogues. For example, the diamond (100) dimer π-bonding energy is approximately 117 kJ/mol while that of ethylene is 234 kJ/mol [7,8]. The π interactions on Si and Ge surface are even weaker, e.g., only 20–40 kJ/mol for Si(100) [9]. These different π-bonding energies suggest that the diamond surface dimer is more reactive than ethylene, but less reactive than Si(100) or Ge(100). Experimental and theoretical studies have shown that the surface dimers of Si(100), Ge(100) and diamond(100) can react with unsaturated organic compounds through [2+2] or [4 + 2] cycloaddition forming four- or six-membered-rings at the surface [10–22]. Such chemical modification offers great opportunities for tailoring physical and chemical properties of these semiconducting materials for specific applications.

Another important cycloaddition reaction is the 1,3-dipolar cycloaddition; for example, the reactions of nitrones with simple alkenes have received great attention in asymmetric synthesis. One of the reasons is that most nitrones are stable compounds that do not require *in situ*

* Corresponding author. Address: School of Chemistry and Chemical Engineering, Shandong University, Jinan, Shandong 250100, China. Tel.: +86 531 8836 5576; fax: +86 531 8856 4464.
E-mail address: yongjunliu_1@sdu.edu.cn (Y. Liu).

0166-1280/$ - see front matter © 2007 Elsevier B.V. All rights reserved.
doi:10.1016/j.theochem.2007.10.023

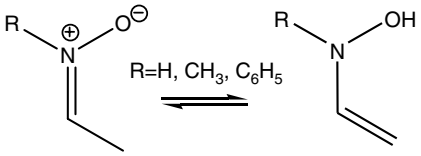

Scheme 1.

formation. On the other hand, the 1,3-dipolar cycloaddition of nitrones can form up to three new contiguous chiral centers and the adducts can be transformed into many other building-block molecules.

Lu et al. have studied the 1,3-dipolar cycloadditions of a series of small 1,3-diploar molecules on the C(100) surface by means of hybrid density functional B3LYP method [23]. They found that all the 1,3-dipolar cycloadditions are more favorable than their molecular analogues both thermodynamically and kinetically, which may be used to modify the diamond surface at low temperature.

To explore a new type of surface reaction that can be used to functionalize diamond surface, the present work provides a theoretical prediction of the 1,3-dipolar cycloaddition of nitrones on the reconstructed C(100)-2 × 1 surface. Nitrones with α-hydrogen and the hydroxylamine tautomers are isomers (see Fig. 1), the latter possess reactive C=C double bonds. Therefore, the reactions of hydroxylamine tautomers with the C(100) surface were also examined.

2. Computation method

All calculations were performed using the Gaussian 03 program package [24]. The geometric parameters of the reactants, intermediates, transition states and adducts were fully optimized at (U)B3LYP [25]/6-31G(d) level and confirmed by vibrational analysis. It has been shown that the B3LYP approach can provide a reliable description for the 1,3-dipolar cycloadditions of a series of small 1,3-diploar molecules on the C(100) surface [23]. On a potential energy surface all optimized geometries correspond to a local minimum that has no imaginary frequency mode or to a saddle point that has only one imaginary frequency mode. The reported energies have been corrected by inclusion of zero-point energies (ZPE) unless otherwise specified explicitly.

We employed a C_9H_{12} cluster model to represent dimer sites on the C(100)-2 × 1 surface, which has been used in the theoretical investigation of addition reactions on diamond surface previously [11d,14a,23].

3. Results and discussion

The most commonly used substituents at the nitrogen atom of nitrone are phenyl or phenylethyl group because it can be removed from the resulting adduct by hydrogenolysis [26,27]. To be simple, we only studied the reactions of nitrone, *N*-methyl nitrone and *N*-phenyl nitrone with the C(100) surface.

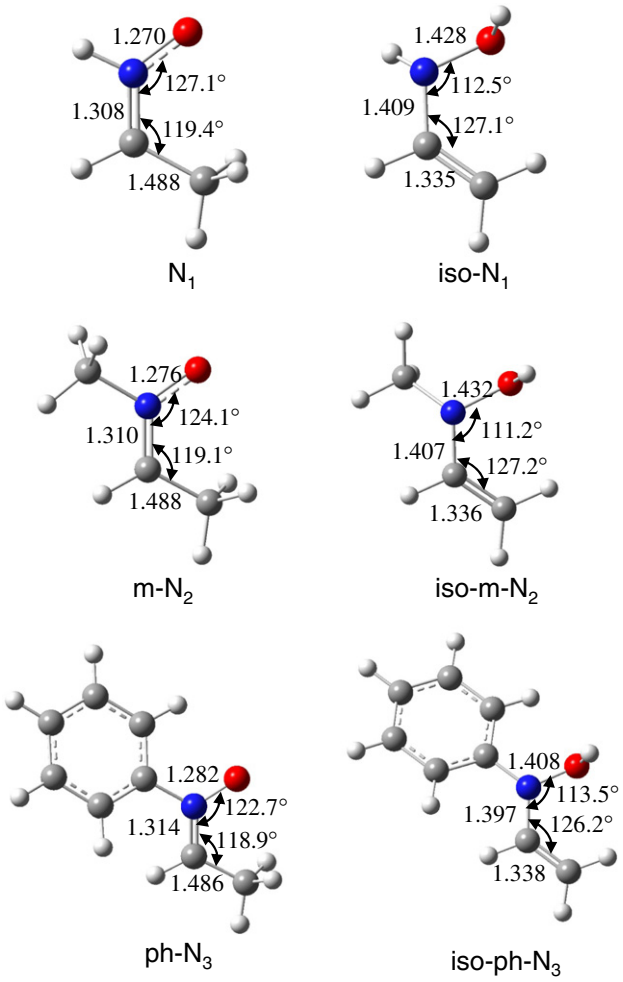

Fig. 1. Structures of nitrone (N_1), *N*-methyl nitrone (m-N_2), *N*-phenyl nitrone (ph-N_3) and their hydroxylamine tautomers vinyl-hydroxylamine (iso-N_1), *N*-methyl-vinyl-hydroxylamine (iso-m-N_2) and *N*-phenyl-vinyl-hydroxylamine (iso-ph-N_3) calculated at B3LYP/6-31G(d) level. Lengths are in 0.1 nm and angles are in degrees.

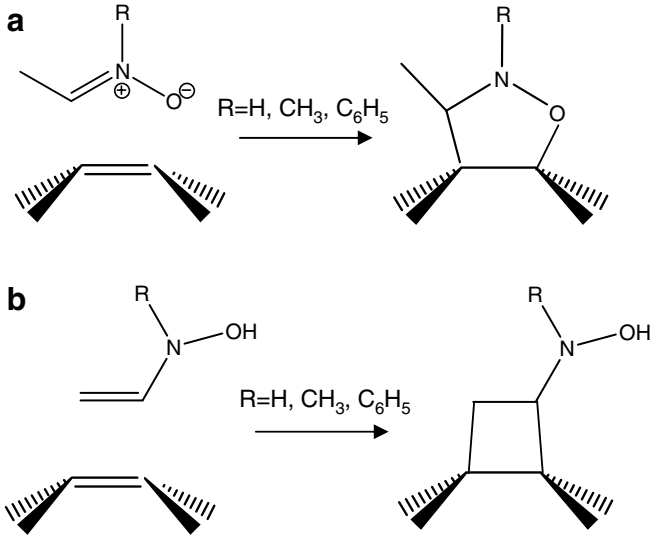

Fig. 2. Possible reaction pathways. (a) 1,3-Dipolar cycloaddition of nitrone, *N*-methyl nitrone and *N*-phenyl nitrone; (b) [2+2] addition reaction of vinyl-hydroxylamine tautomers.

Our previous studies have shown that nitrones could undergo isomerization to form their hydroxylamine tautomers [28]. The optimized structures of nitrone (N_1), *N*-methyl nitrone (m-N_2), *N*-phenyl nitrone (ph-N_3) and their hydroxylamine tautomers (denoted as iso-N_1, iso-m-N_2, and iso-ph-N_3, respectively) are shown in Fig. 1.

Nitrone (N_1), *N*-methyl nitrone (m-N_2) and *N*-phenyl nitrone (ph-N_3) are typical 1,3-dipoles, which can undergo 1,3-dipolar cycloaddition. Their hydroxylamine tautomers possess C=C double bonds (that can be described as ethylene derivatives), which could react with the C(100) surfaces as well. Therefore, in this study, two kinds of reactions on the diamond (100) were considered: (1) 1,3-dipolar cycloaddition of the nitrones and (2) [2+2] cycloaddition reaction of the hydroxylamine tautomers, as shown in Fig. 2.

3.1. 1, 3-dipolar cycloaddition of nitrones

The optimized structures of the transition states ($TS_{1,1}$, $TS_{2,1}$ and $TS_{3,1}$) and products ($P_{1,1}$, $P_{2,1}$ and $P_{3,1}$) for the 1,3-dipolar cycloadditions of nitrone, *N*-methyl nitrone and *N*-phenyl nitrone with the C(100)-2 × 1 surface are shown in Fig. 3. Their energy profiles are drawn in Fig. 4.

As shown in Fig. 3, the lengths of the two newly forming bonds in the transition states are not deviated from each other significantly. Therefore, the 1,3-dipolar cycloaddition reactions of nitrones with the C(100) surface follow concerted reaction mechanism, which agrees well with most of the 1,3-dipolar cycloaddition reactions on the C(100) surface [23]. Vibrational analysis indicated that the two transition states correspond to unique imaginary frequencies (135.3*i* cm^{-1} for $TS_{1,1}$, 176.3*i* cm^{-1} for $TS_{2,1}$ and 122.8*i* cm^{-1} for $TS_{3,1}$) and can be affirmed as real ones. Calculations of intrinsic reaction coordinates (IRC) and further optimization of the primary IRC results revealed that the transition states "bridge" the reactants and adducts.

Fig. 3 also showed that the transition states ($TS_{1,1}$, $TS_{2,1}$ and $TS_{3,1}$) are formed very early since the bond lengths of the two new bonds are very long compared with the products ($P_{1,1}$, $P_{2,1}$ and $P_{3,1}$). This type of reaction usually associates with a smaller reaction barrier but a larger exothermicity [29]. As shown in Fig. 4, the 1,3-dipolar cycloaddition of nitrones to diamond (100) surface proceeds with a very small activation barrier (less than 12 kJ/mol).

In our previous studies [28], we have investigated the reaction mechanism of 1,3-dipolar cycloaddition of nitrone and *N*-methyl nitrone on the Si(100) surface. We found no evidence for an activation barrier between the separated reactants and the 1,3-dipolar cycloaddition adducts, which is different from the present study. We ascribe it to the different bond strengths of Si=Si and C=C dimers. The

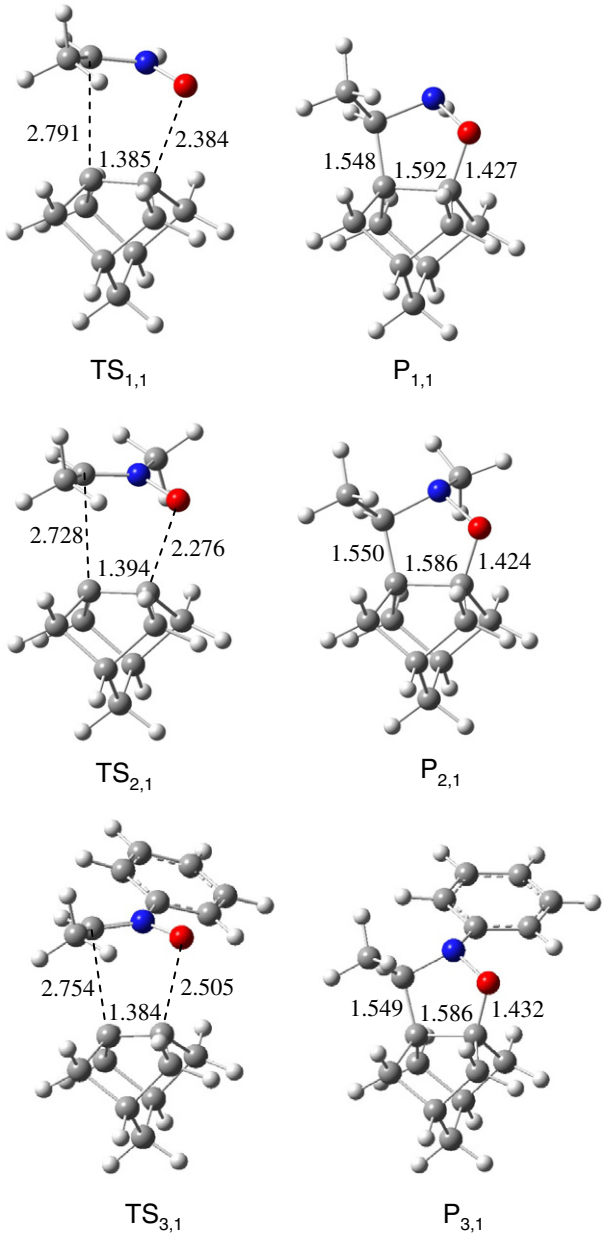

Fig. 3. Optimized geometric structures for transition states ($TS_{1,1}$, $TS_{2,1}$ and $TS_{3,1}$) and product ($P_{1,1}$, $P_{2,1}$ and $P_{3,1}$) for the 1,3-dipolar cycloaddition reactions. Lengths are in 0.1 nm.

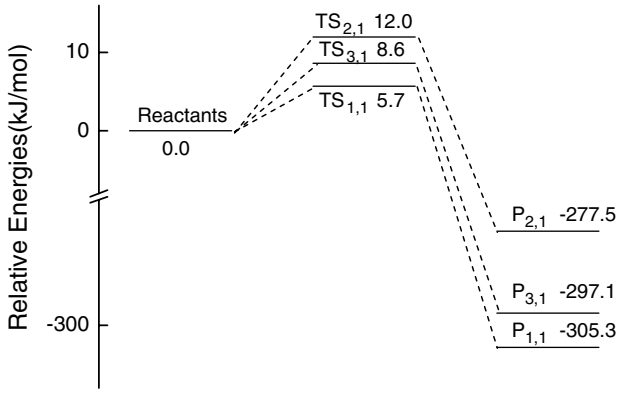

Fig. 4. Energy profile for the 1,3-dipolar cycloaddition reaction of nitrone (N_1), *N*-methyl nitrone (m-N_2), and *N*-phenyl nitrone (ph-N_3) with C_9H_{12} at B3LYP/6-31G(d) level.

π-bonding in Si dimer is much weaker than that of C dimer, so that there is little energy cost to overcome a barrier before the surface can form a bond to the incoming molecules. In addition, the initial stage of the 1,3-dipolar

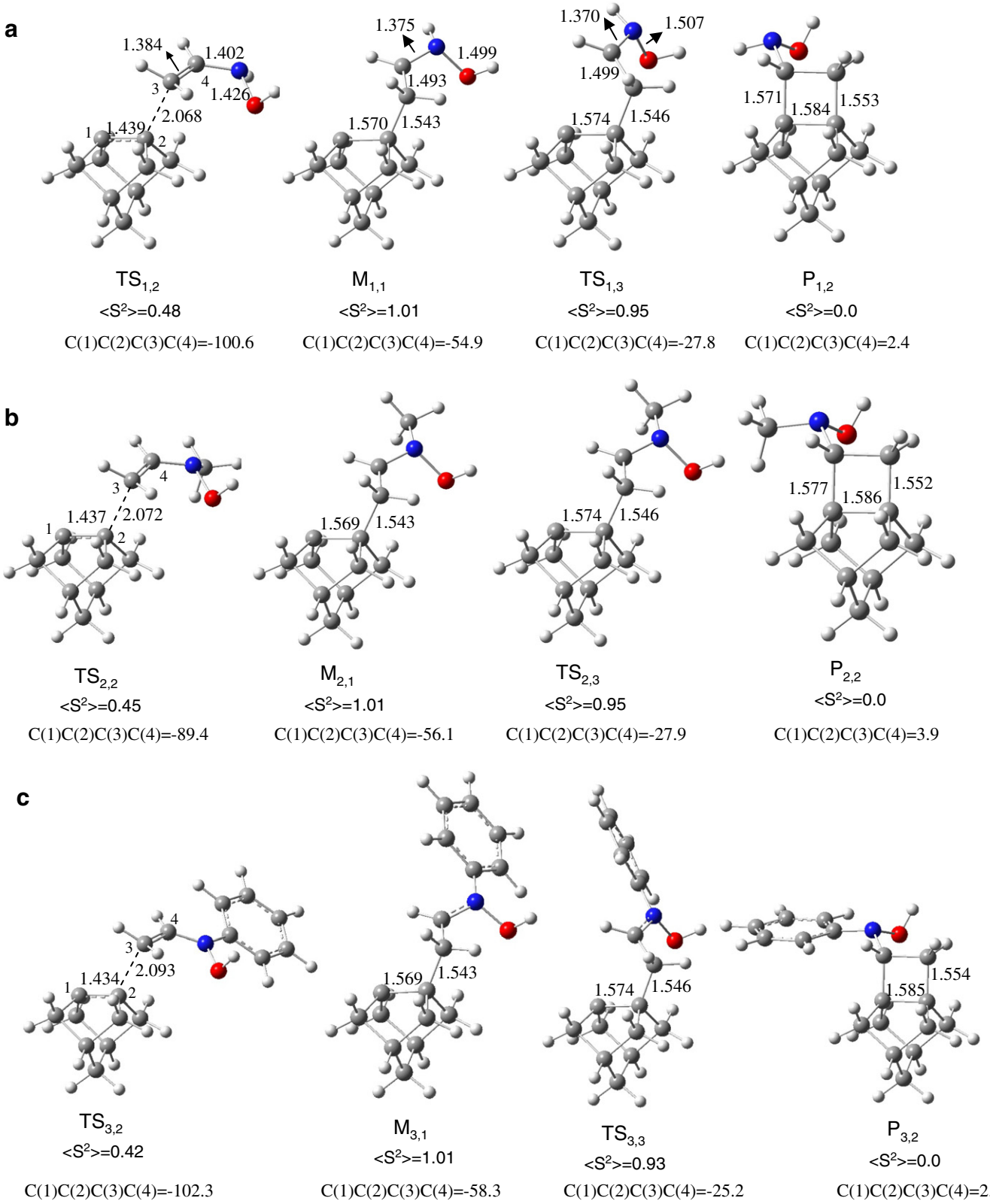

Fig. 5. UB3LYP/6-31G(d) optimized geometric structures for the [2+2] cycloaddition reactions of vinyl-hydroxylamine tautomers. (a) Transition state ($TS_{1,2}$), intermediate ($M_{1,1}$), transition state ($TS_{1,3}$) and product ($P_{1,2}$); (b) transition state ($TS_{2,2}$), intermediate ($M_{2,1}$), transition state ($TS_{2,3}$) and product ($P_{2,2}$); (c) transition state ($TS_{3,2}$), intermediate ($M_{3,1}$), transition state ($TS_{3,3}$) and product ($P_{3,2}$). Lengths are in 0.1 nm and angles are in degrees. The values of $\langle S^2 \rangle$ for the wave functions of these stationary are also given.

addition of nitrones on the Si(100) surface involves the formation of a Si—O bond. Since the Si—O bond energy (108 kcal/mol) is much larger than that of C—O bond (86 kcal/mol) [30], the formation of Si—O bond lowers the barrier more effectively. Therefore, the reaction with the Si(100) surface is more facile than with the diamond (100) surface.

3.2. [2+2] cycloaddition of hydroxylamine tautomers

Our calculations predicted that the addition reactions of hydroxylamine tautomers with the C(100)-2 × 1 surface follow a stepwise mechanism. The geometrical feature of the transition states, intermediates and products are shown in Fig. 5. The energy profiles of the reaction paths are shown in Fig. 6.

As shown in Figs. 5 and 6, the rate-determining step for the [2+2] cycloaddition reaction is the formation of a diradical intermediate ($M_{1,1}$, $M_{2,1}$ or $M_{3,1}$) but not the ring-closing step. The activation barrier energies for the formation of diradical intermediates $M_{1,1}$, $M_{2,1}$ and $M_{3,1}$ are 57.4, 55.8 and 51.1 kJ/mol, respectively. In the diradical intermediates, the hydroxylamine moiety is mono-σ bonded to a C dimer atom. From $M_{1,1}$, $M_{2,1}$ and $M_{3,1}$ ring-closing to form the final products, $P_{1,2}$, $P_{2,2}$ and $P_{3,2}$, this process is slightly activated with a negligible barrier of 2.8, 3.7 and 4.2 kJ/mol corresponding to the transition state $TS_{1,3}$, $TS_{2,3}$ and $TS_{3,3}$, respectively.

From Fig. 5a, one can see that the dihedral C(1)—C(2)—C(3)—C(4) increases from −100.6 (in $TS_{1,2}$) to 2.4° (in $P_{1,2}$) along the reaction pathway. From $M_{1,1}$ to $TS_{1,3}$, the main change of the geometry is the internal rotation of hydroxylamine moiety around C(2)—C(3) bond. The reactions of *N*-methyl-vinyl-hydroxylamine (iso-m-N_2) and *N*-phenyl-vinyl-hydroxylamine (iso-ph-N_3) show the same cases. Because of the small barrier height of $TS_{1,3}$, $TS_{2,3}$ and $TS_{3,3}$, the ring-closing reactions of $M_{1,1}$, $M_{2,1}$ and $M_{3,1}$ could occur very easily (see Fig. 6).

In our previous study [28], we have investigated the [2+2] cycloaddition reaction of vinyl-hydroxylamine (iso-N_1) and *N*-methyl-vinyl-hydroxylamine (iso-m-N_2) on the Si(100)-2 × 1 surface. Calculations revealed that the reactions follow a π-complex (intermediate) mechanism. The Si=Si double bond of vinyl-hydroxylamine first forms a π-complex (intermediate) with barrier-free reactions, the intermediate then undergoes a ring-closing reaction to form the final product. A small energy barrier must be overcome to form the final product, which is different from the reactions on the C(100) surface. Large barriers are encountered in the formation of the diradical intermediates, which may result from the different π-bond strengths of Si=Si and C=C dimers.

Furthermore, the $\langle S^2 \rangle$ values for the wave functions of stationary points are calculated at UB3LYP/6-31G(d) level (see Fig. 5). The values of $\langle S^2 \rangle$ for $M_{1,1}$, $M_{2,1}$, $M_{3,1}$, $TS_{1,3}$, $TS_{2,3}$ and $TS_{3,3}$ are ~1.0, indicating that the structures are half singlet and half triplet and that the present DFT calculations exhibit large spin contaminations [31]. The use of multi-configuration methods has been demonstrated to be a simple way to obtain more accurate configuration predictions on the entire potential energy surface [31]. Therefore, for comparison, CASSCF (complete active space SCF) wave functions were used to describe the stationary points (intermediates and transition states) on the reaction pathway of vinyl-hydroxylamine (iso-N_1).

In the CASSCF calculation, a (4,4) active space was used. The optimized structures are shown in Fig. 7a. For the study of $TS_{1,4}$, the active space is constructed from

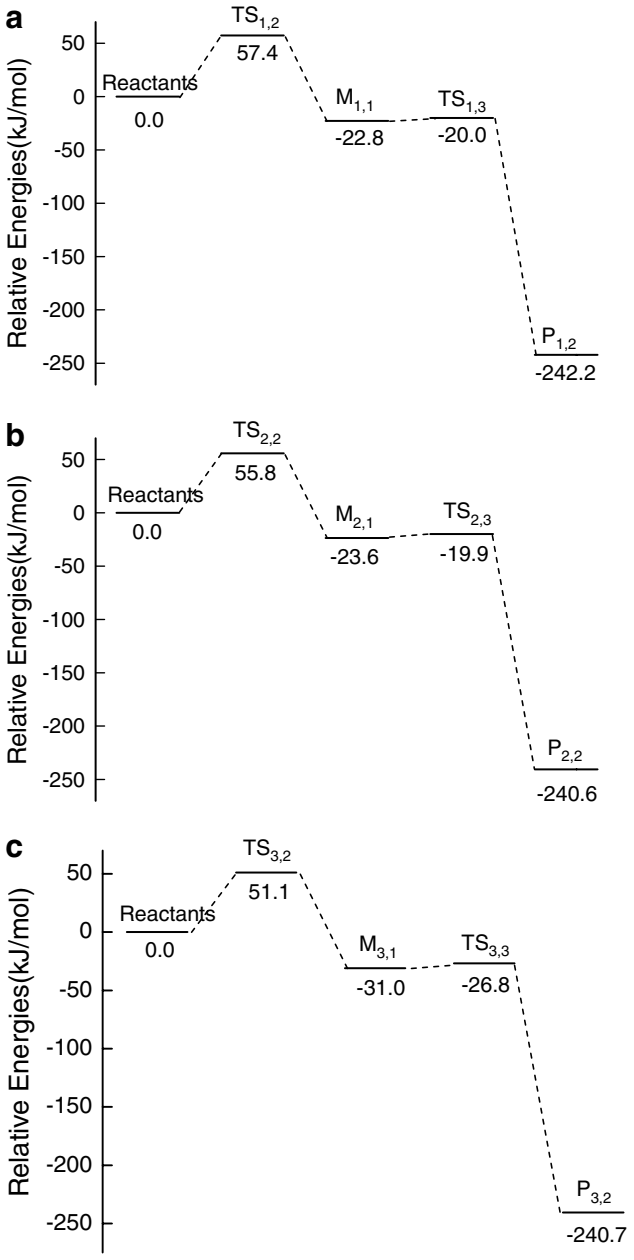

Fig. 6. Energy profile for the [2+2] cycloaddition reaction at UB3LYP/6-31G(d) level. (a) Vinyl-hydroxylamine (iso-N_1) with C_9H_{12}; (b) N-methyl-vinyl-hydroxylamine (iso-m-N_2) with C_9H_{12}; (c) *N*-phenyl-vinyl-hydroxylamine (iso-ph-N_3) with C_9H_{12}.

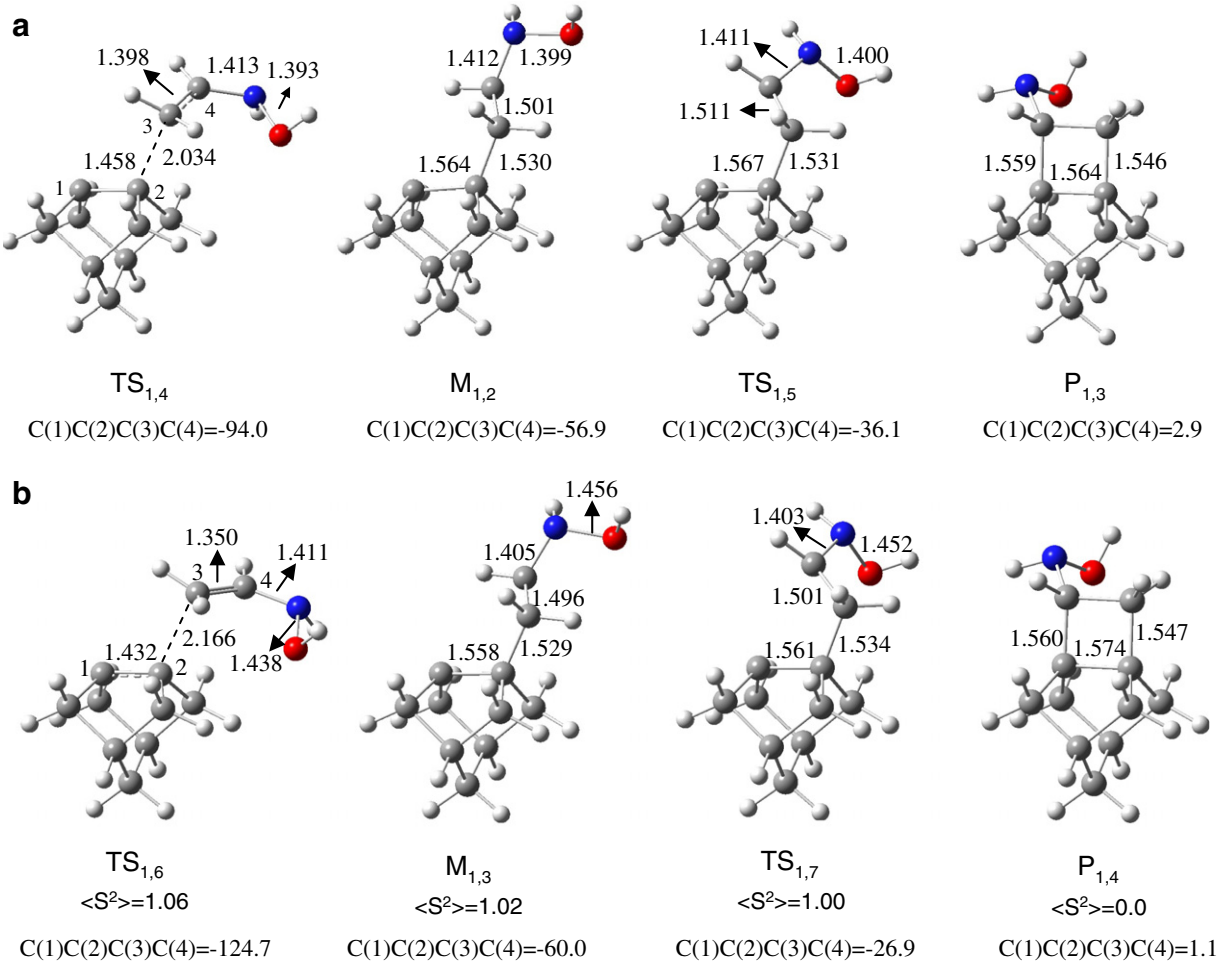

Fig. 7. (a) CASSCF optimized geometric structures of transition state ($TS_{1,4}$), intermediate ($M_{1,2}$), transition state ($TS_{1,5}$) and product ($P_{1,3}$) for [2+2] cycloaddition of nitrone; (b) MP2 optimized geometric structures of transition state ($TS_{1,6}$), intermediate ($M_{1,3}$), transition state ($TS_{1,7}$) and product ($P_{1,4}$) for [2+2] cycloaddition of nitrone. Lengths are in 0.1 nm and angles are in degrees.

the two electrons in π and π* orbitals of the surface C dimer and two electrons in π and π* orbitals of the C═C bond. For the study of $M_{1,2}$ and $TS_{1,5}$, the active space is constructed from the unpaired two electrons of C(1) and C(4) in p (occupied) and p (unoccupied) orbitals and the two electrons in σ and σ* orbitals of C(2)—C(3) bond.

Fig. 7a shows that the CASSCF calculated structures are similar to those of the DFT results besides the moiety of vinyl-hydroxylamine. The difference in the moiety of vinyl-hydroxylamine is due to the diradical nature of the intermediate and transition state. The active apace NOON (natural orbital occupation number) values for the active space of $M_{1,2}$ are 1.999, 0.9075, 1.092 and 0.000. This clearly indicated a diradical state. The large diradical character suggests the previous DFT calculations suffered from large spin contaminations.

The CASSCF energy profile is shown in Fig. 8a. As the CASSCF results indicated, the rate-determining step is the formation of the diradical intermediate, not the ring-closing step. The activation barrier height for the formation of the diradical intermediates is 111.0 kJ/mol, which is much larger than that of B3LYP results. From $M_{1,2}$ ring-closing to form the final product, $P_{1,3}$ is slightly activated with barrier of 8.4 kJ/mol at transition state $TS_{1,5}$.

Furthermore, the Møller–Plesset second-order perturbation (MP2) method was used to re-optimize the stationary points (intermediates and transition states) on the reaction pathway of vinyl-hydroxylamine (iso-N_1) with the C(100) surface to check out the validity of the methods. The optimized structures are shown in Fig. 7b. From Fig. 7b, one can see that the MP2 optimized structures are similar to those of CASSCF and DFT results.

The MP2 energy profile is shown in Fig. 8b. Although the relative energies of the stationary points are different between MP2, CASSCF and DFT methods, they give the same qualitative results.

4. Conclusions

The mechanism of the reaction between nitrone, *N*-methyl nitrone, *N*-phenyl nitrone, together with their hydroxylamine tautomers (vinyl-hydroxylamine, *N*-methyl-vinyl-hydroxylamine, *N*-phenyl-vinyl-hydroxylamine) and the reconstructed C(100)-2 × 1 surface has

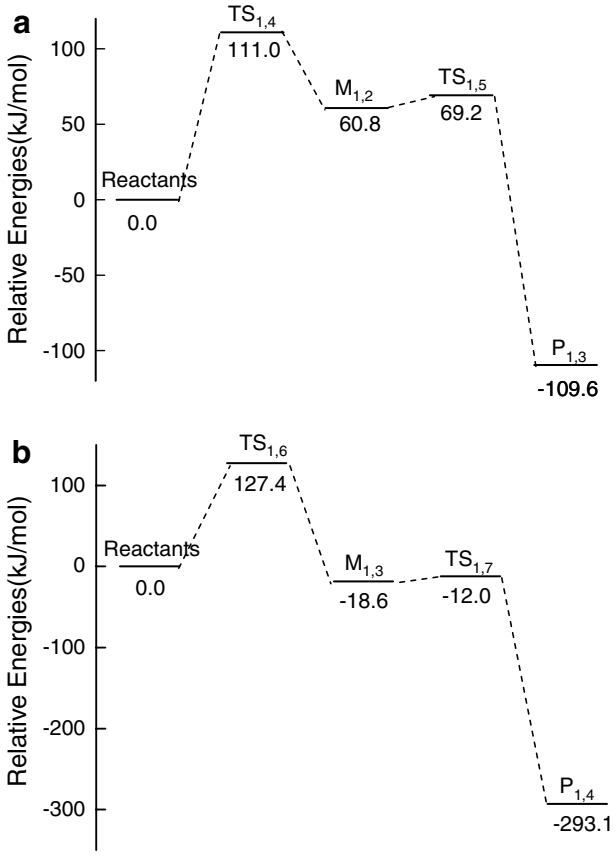

Fig. 8. Energy profile for the [2+2] cycloaddition reaction of nitrone. (a) CASSCF/6-31G(d) method; (b) MP2 method. The energies are ZPE-uncorrected.

been studied by using the hybrid density functional theory (B3LYP), multi-configuration complete-active-space self-consistent-field (CASSCF) and Møller–Plesset second-order perturbation (MP2) methods. The calculations predicted that the nitrones can react with the surface dimer via facile 1,3-dipolar cycloaddition reaction with small activation barriers (less than 12.0 kJ/mol). The [2+2] cycloaddition of hydroxylamine tautomers on the C(100) surface follows a diradical mechanism. Hydroxylamine tautomers first form diradical intermediates by overcoming large activation barrier of 50–60 kJ/mol (B3LYP), then generate the [2+2] cycloaddition products through diradical transition states with negligible activation barriers. Because of the larger barrier of the [2+2] cycloaddition, the favored reaction of nitrone with the C(100) surface is 1,3-dipolar cycloaddition.

Acknowledgements

This work was supported by the Scientific Research Foundation for the Returned Overseas Chinese Scholars (State Education Ministry) and the Program of Hundreds Talent of the Chinese Academy of Science.

Appendix A. Supplementary data

Supplementary data associated with this article can be found, in the online version, at doi:10.1016/j.theochem.2007.10.023.

References

[1] G.S. Gildenblat, S.A. Grot, A. Badzian, Proc. IEEE 79 (1991) 647.
[2] J.E. Field, The Properties of Natural and Synthetic Diamond, Academic Press, London, 1992.
[3] C. Yang, H.C. Kang, Surf. Sci. 409 (1998) 521.
[4] B.D. Thoms, J.E. Butler, Surf. Sci. 328 (1995) 291.
[5] T.W. Mercer, P.E. Pehrsson, Surf. Sci. 399 (1998) L327.
[6] M.P Develyn, in: Handbook of Industrial Diamonds and Diamond films, Dekker, New York, 1998.
[7] T.I. Hukka, T.A. Pakkanen, M.P. D'Evelyn, J. Phys. Chem. 98 (1994) 12420.
[8] J. McMurry, Organic Chemistry, Fourth ed., Brooks/Cole Publishing Company, Pacfic Grove, 1996.
[9] D.J. Doren, Adv. Chem. Phys. 95 (1996) 1.
[10] (a) J.S. Hovis, S.K. Coutler, R.J. Hamers, M.P. D'Evelyn, J.N. Russell, J.E. Butler, J. Am. Chem. Soc. 122 (2000) 732;
(b) J.S. Hovis, H. Liu, R.J. Hamers, J. Phys. Chem. B 102 (1998) 6873.
[11] (a) R. Konečný, D.J. Doren, Surf. Sci. 417 (1998) 169;
(b) R. Konečný, D.J. Doren, J. Am. Chem. Soc. 119 (1997) 11098;
(c) J.A. Barriocanal, D.J. Doren, J. Am. Chem. Soc. 123 (2001) 7340;
(d) D.R. Fitzgerald, D.J. Doren, J. Am. Chem. Soc. 122 (2002) 12334.
[12] Q. Liu, R. Hoffmann, J. Am. Chem. Soc. 117 (1995) 4082.
[13] (a) C.H. Chio, M.S. Gordon, J. Am. Chem. Soc. 124 (2002) 6162;
(b) H.S. Lee, C.H. Chio, M.S. Gordon, J. Phys. Chem. B 109 (2005) 5067;
(c) Y. Jung, M.S. Gordon, J. Am. Chem. Soc. 127 (2005) 3131.
[14] (a) X. Lu, M. Zhu, X. Wang, J. Phys. Chem. B 108 (2004) 7359;
(b) X. Lu, J. Am. Chem. Soc. 125 (2003) 6384;
(c) X. Lu, M. Zhu, X. Wang, Q. Zhang, J. Phys. Chem. B 108 (2004) 4478.
[15] L.C. Teague, D.J. Chen, J.J. Boland, J. Phys. Chem. B 108 (2004) 7827.
[16] G.P. Lopinski, D.J. Moffatt, D.D.M. Wayner, R.A. Wolkov, J. Am. Chem. Soc. 122 (2000) 3548.
[17] P. Minary, M.E. Tuckerman, J. Am. Chem. Soc. 127 (2005) 1110.
[18] (a) Y. Wang, J. Ma, S. Inagaki, Y. Pei, J. Phys. Chem. B 109 (2005) 5199;
(b) Y. Wang, J. Ma, J. Phys. Chem. B 110 (2006) 5542.
[19] (a) A.V. Teplyakov, M.J. Kong, S.F. Bent, J. Am. Chem. Soc. 119 (1997) 11100;
(b) A.V. Teplyakov, P. Lal, Y.A. Noah, S.F. Bent, J. Am. Chem. Soc. 120 (1998) 7377.
[20] R.J. Hamers, J.S. Hovis, C.M. Greenlief, D.F. Padowitz, Jpn. J. Appl. Phys. 38 (1999) 3879.
[21] Y. Okamota, J. Phys. Chem. B 105 (2001) 1813.
[22] G.T. Wang, S.F. Bent, J. Am. Chem. Soc. 122 (2000) 744.
[23] (a) X. Lu, X. Xu, N. Wang, Q. Zhang, J. Org. Chem. 67 (2002) 515;
(b) X. Lu, X. Xu, N. Wang, Q. Zhang, J. Phys. Chem. B 106 (2002) 5972;
(c) X. Lu, G. Fu, N. Wang, Q. Zhang, M.C. Lin, Chem. Phys, Lett. 343 (2001) 212.
[24] M.J. Frisch et al., Gaussian 03, Revision C.02, Gaussian, Inc. Wallingford, CT, 2004.
[25] A.D. Becke, J. Chem. Phys. 98 (1993) 5648.
[26] K.V. Gothelf, K.A. Jørgensen, Chem. Rev. 98 (1998) 863.
[27] M. Arnó, R.J. Zaragozá, L.R. Domingo, Tetrahedron: Asymmetry 15 (2004) 1541.
[28] Y. Liu, Z. Wang, J. Phys. Chem. C 111 (2007) 4673.
[29] G.S. Hammond, J. Am. Chem. Soc. 77 (1954) 334.
[30] J. Emsley, The Elements, Clarendon Press, Oxford, UK, 1993.
[31] H.S. Lee, C.H. Choi, M.S. Gordon, J. Phys. Chem. B 109 (2005) 5067.